JOURNAL OF MATERIALS SCIENCE 25 (1990) 1–5

Formation temperature of bosons in high-T_c $YBa_2Cu_3O_{7-y}$ systems

Y. NISHI, A. IGARASHI, S. MORIYA, N. NINOMIYA, S. TOKUNAGA
Department of Materials Science, Tokai University, 1117 Kitakaname, Hiratsuka, Kanagawa, Japan

At different equilibrium temperatures, a precise measurement of the electrical resistivity (R) is performed for high T_c polycrystalline $YBa_2Cu_3O_{7-y}$ systems. T^2 law is applied in the part of the R–T relationship far above the superconducting transition temperature. Since Landau and Pomeranchuk predicted the T^2 law arising from electron–electron scattering, a higher critical temperature of T^2 law is defined as a start point (T_{es}) of electron–electron scattering. On the other hand, we defined a lower critical temperature of T^2 law as the formation temperature (T_{ee}) of an electron–electron pair, i.e. the formation temperature of boson. T_{ee} relates to the offset temperature of the superconducting transition ($T_{c_{off}}$).

1. Introduction

Several workers have reported high superconducting transition temperatures above boiling point (b.p.) of N_2 for the Y–Ba–Cu–O oxide [1–5]. It is important to suggest a new model of superconducting transition. Since an electron–phonon coupling of the BCS model [6] might be partially inapplicable for high T_c materials, new models, which are suggested to be electron–electron pairs and groups such as an exciton mechanism, have been proposed [7–9]. A law of T^2, which is the temperature dependence of electrical resistivity, was applied for Li, Na, K and Ag at extremely low temperature [10–12]. Landau and Pomeranchuk predicted the law from electron–electron scattering [13]. If some new models were applied for the high T_c of the Y–Ba–Cu–O system, the T^2 law would be found at high temperature. We found the T^2 law of the temperature dependence of the electrical resistivity above the onset temperature of the transition for the high T_c polycrystalline Y–Ba–Cu–O system [14]. We define a lower critical temperature of T^2 law as the formation temperature (T_{ee}) of boson. At T_{ee} the electron–electron pair converts to the boson instead of scattering. The purpose of the present work is to investigate the relationship between T_{ee} and $T_{c_{off}}$ for the high T_c polycrystalline Y–Ba–Cu–O system.

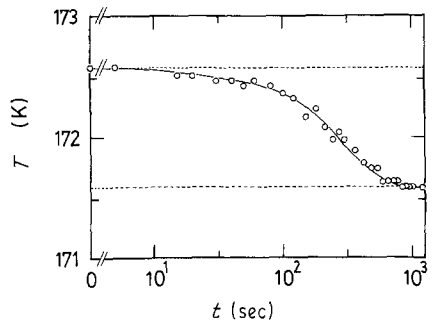

Figure 1 Change in temperature with time. Equilibrium temperature is taken at about 1000 sec.

2. Sample preparation

Samples with nominal composition $YBa_2Cu_3O_{7-y}$ were prepared from high purity powders of CuO, $BaCO_3$ and Y_2O_3. The powders were mixed and reacted at 1200 K in air and then air-cooled. After crushing, the pelletized tablet, 2 mm thick, 23 mm diameter, was sintered in air at 1200 K and furnace-cooled. The cooling rate was 7.0×10^{-2} K sec^{-1}. Experimental conditions of sample preparation, lattice constants and results are summarized in Table I.

3. Electrical resistivity change with temperature

Electrical resistivity was measured using a standard four-probe technique and a Keithley 181 nanovoltmeter. The temperature was measured by Au*Fe–chromel thermocouple attached to the specimen in a cryostat at equilibrium temperatures. Figure 1 shows temperature change with cooling time. Since the value of the resistivity depends on the scanning rate of the cryostat (see Fig. 2), the most important point is a precise measurement of the electrical resistivity at equilibrium temperatures.

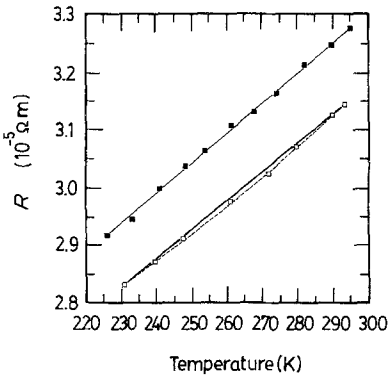

Figure 2 Change in electrical resistivity (R) with temperature (T) of $YBa_2Cu_3O_{7-y}$ system. (□) is for the measurement at equilibrium temperature; (■) is for the measurement on continuous cooling conditions (scanning rate is 0.12 K sec^{-1}).

0022–2461/90 $03.00 + .12

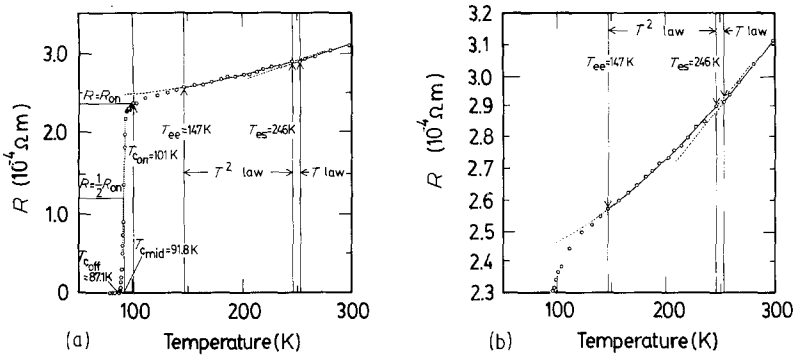

Figure 3 Change in electrical resistivity (R) with temperature (T) of $YBa_2Cu_3O_{7-y}$ system.

Figure 3 shows the temperature dependence of electrical resistivity of the high T_c $YBa_2Cu_3O_{7-y}$ oxide. The lower the temperature, the lower the electrical resistivity becomes. An apparent deviation occurs at a temperature between 101 and 147 K. There is a sharp drop between 87.1 and 101 K. Offset, $T_{c_{off}}$, of the transition is defined as the temperature corresponding to the achievement of zero-resistivity (below 10^{-9} Ωm). Onset, $T_{c_{on}}$, of the transition is defined as the temperature corresponding to the achievement of the deviation of the electrical resistivity. Namely, $T_{c_{on}}$ is taken as the temperature at $dR/dT = 0.03xR^{300\,K}$, where dR/dT and $R^{300\,K}$ are the slope of R–T and the resistivity at 300 K, respectively. The midpoint is designated $T_{c_{mid}}$. The $T_{c_{off}}$ and $T_{c_{mid}}$ values of the $YBa_2Cu_3O_{7-y}$ system are 87.1 and 91.8 K, respectively.

4. T^2 law

It is traditional to express the total electrical resistivity R as the sum of two terms:

$$R = R_0 + R(T) \quad (1)$$

Here $R(T)$ is the temperature dependent term arising from the dynamic deviations from crystal perfection. R_0 is the temperature independent residual resistivity arising from the static imperfections, such as impurities and lattice defects. $R(T)$ relates to temperature (T) as in the following equations:

$$R(T) = A_{ep}T \text{ (at high temperature)} \quad (2)$$

$$R(T) = A_{ee}T^2 \text{ (at low temperature)} \quad (3)$$

Here A_{ep} and A_{ee} are constants. Equation 2 is applied for metals near room temperature and is dominated by electron–phonon scattering. Equation 3 is applied for alkali and noble metals at extremely low temperature [10–12]. Since the effect of the electron–phonon scattering is small at low temperature, Equation 3 is dominated by the electon–electron scattering. Figures 4a and b show change in R with T^2 for the high T_c (above 90 K) Y–Ba–Cu–O oxide. Although the temperature is not low, we find that Equation 3 applies far above the superconducting transition temperature. Landau and Pomeranchuk predicted

TABLE I Experimental conditions of sample preparation

Sample no.	Volume fraction (x)	Preparation				Measurement conditions		
		Temp. (K)	Time (h)	FA	CR (K sec^{-1})	Cross-sectional area (m^2)	CD (A m^{-2})	TD (mm)
A-1	0	1200	(2, 8)	air	7×10^{-2}	3.69×10^{-6}	271	0.829
A-2	0	1200	(2, 8)	air	7×10^{-2}	3.69×10^{-6}	271	0.758
A-3	0	1200	(0. 10)	air	7×10^{-2}	4.04×10^{-6}	1000	0.797
A-4	0	1173	(3, 24)	air	7×10^{-2}	6.01×10^{-6}	200	0.354
A-5	0	1200	(2, 8)	air	7×10^{-2}	6.08×10^{-6}	200	1.974
A-6	0	1200	(3, 24)	air	7×10^{-2}	2.55×10^{-6}	1003	3.812
A-7	0	1200	(3, 24)	air	7×10^{-2}	2.73×10^{-6}	1004	2.725
A-8	0	1200	(3, 24)	air	7×10^{-2}	2.45×10^{-6}	1001	6.402
B-1	0.01 (Pd)	1200	(0, 10)	air	7×10^{-2}	4.09×10^{-6}	200	1.194
B-2	0.005 (Pd)	1200	(0, 10)	air	7×10^{-2}	4.41×10^{-6}	200	1.359
B-3	0.001 (Pd)	1200	(0, 10)	air	7×10^{-2}	7.76×10^{-6}	200	0.350
B-4	0.0001 (Pd)	1200	(0, 10)	air	7×10^{-2}	4.48×10^{-6}	200	0.498
C-1	0.1 (Ti)	1200	(0, 10)	air	7×10^{-2}	6.02×10^{-6}	200	0.683
C-2	0.01 (Ti)	1200	(0, 10)	air	7×10^{-2}	6.12×10^{-6}	200	0.681
C-3	0.001 (Ti)	1200	(0, 10)	air	7×10^{-2}	5.54×10^{-6}	200	0.756
C-4	0.0001 (Ti)	1200	(0, 10)	air	7×10^{-2}	8.07×10^{-6}	200	0.522
C-5	0.00001 (Ti)	1200	(0, 10)	air	7×10^{-2}	4.56×10^{-6}	200	1.660
D-1	0	1200	(2, 8)	air	7×10^{-2}	3.69×10^{-6}	271	0.604
D-2	0	1200	(2, 8)	air	7×10^{-2}	3.69×10^{-6}	271	0.649
D-3	0	1200	(2, 8)	air	7×10^{-2}	3.69×10^{-6}	271	0.531

FA; furnace atmosphere
CR; cooling rate
CD; current density
TD; terminal distance

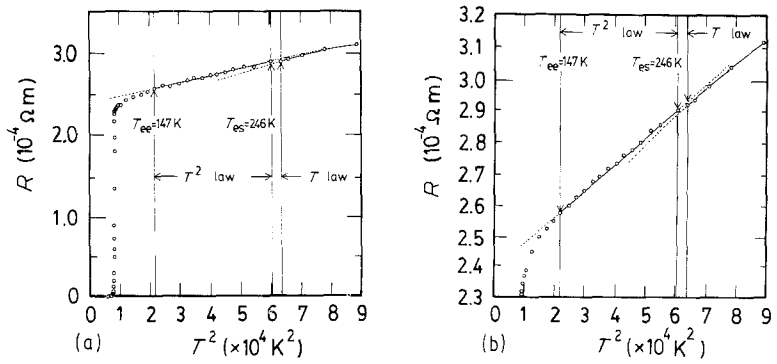

Figure 4 Change in electrical resistivity (R) with T^2 of $YBa_2Cu_3O_{7-y}$ system.

Equation 3 arising from the electron–electron scattering [13]. Figure 5a shows a schematic drawing of the scattering. At the same time of the collision of the electrons, both the electrons should be at the same energy level below Fermi level, although the pairing time is short.

If the scanning rate is high (see Figs 1 and 6) as usually occurs, the T^2 law cannot be found and Equation 2 is applied just above the superconducting transition. Therefore, the most important point at which to measure the electrical resistivity is at equilibrium temperature.

5. Formation temperature (T_{ee}) of boson

Figure 5b shows a schematic drawing of the electron–electron pairing. The electron–electron pair (fermion) converts to boson at T_{ee} in Figs 3 and 4, although the electron–electron scattering is found above T_{ee}. Figure 5c shows a schematic drawing of the boson far below T_{ee} near $T_{c_{off}}$. Many bosons form at E_0 of energy level. Thus, the R change does not apply for the T^2 law below T_{ee} (see Fig. 4). If T_{ee} is the formation temperature of a boson, T_{ee} change should agree with T_c change. In other words, the higher the T_{ee}, the higher the T_c may become. T_{ee} is summarized in Table II.

Figure 7 shows the $T_{c_{off}}$ change with T_{ee} for $YBa_2Cu_3O_{7-y}$ systems in various conditions [15–18]. The higher the T_{ee}, the higher the T_c becomes. Although the work was investigated by use of different kinds of CuO powders under different heat treatments, the $T_{c_{off}}$–T_{ee} relation may be applied as a general rule. $T_{c_{off}}$ is expressed by the following equation:

$$T_{c_{off}} = 0.087T_{ee} + 74.9 \quad (4)$$

Figure 8 shows T_{ee} change with Pd and Ti additions. The small amount of added solutes increases T_{ee}. The maximum T_{ee} for Pd and Ti is 190 and 204 K at $x = 10^{-3}$, respectively (where x is the volume fraction added). We have investigated the effects of Pd and Ti additions on $T_{c_{off}}$ [16, 17]. Figure 9 shows change in $T_{c_{off}}$ with Pd and Ti additions. Small amounts of Pd and Ti additions increase $T_{c_{off}}$. The maximum $T_{c_{off}}$ for Pd and Ti are 92.0 and 93.0 K at $x = 10^{-3}$, respectively. Excess additions of Pd and Ti decrease $T_{c_{off}}$. The T_{ee} change is consistent with the $T_{c_{off}}$ change. Figure 10 shows $T_{c_{off}}$ change with T_{ee}. $T_{c_{off}}$ is expressed by the

TABLE II Results of off set temperature ($T_{c_{off}}$), formation temperature of boson (T_{ee}) and lattice constant

Sample no.	$T_{c_{off}}$ (K)	T_{ee} (K)	X-ray diffraction analysis				
			CS	Lattice constant (nm)			OC
				a	*b*	*c*	
A-1	89.2	165	–	–	–	–	–
A-2	89.0	164	–	–	–	–	–
A-3	88.0	158	ortho	0.3895	0.3823	1.1684	6.79
A-4	87.1	147	ortho	–	–	–	–
A-5	92.0	190	ortho	0.3894	0.3830	1.1712	6.66
A-6	86.5	130	–	–	–	–	–
A-7	85.8	122	–	–	–	–	–
A-8	90.4	181	–	–	–	–	–
B-1	87.0	122	ortho	0.3895	0.3825	1.1686	6.88
B-2	90.0	180	ortho	0.3893	0.3826	1.1678	6.82
B-3	92.0	190	ortho	0.3876	0.3811	1.1629	6.88
B-4	89.0	190	ortho	0.3883	0.3818	1.1649	6.96
C-1	79.0	108	ortho	0.3891	0.3833	1.1672	6.85
C-2	91.0	173	ortho	0.3888	0.3820	1.1665	6.89
C-3	93.0	204	ortho	0.3889	0.3823	1.1666	6.88
C-4	90.0	176	ortho	0.3893	0.3826	1.1679	6.82
C-5	89.0	167	ortho	–	–	–	–
D-1	90.3	168	–	–	–	–	–
D-2	91.5	171	–	–	–	–	–
D-3	93.7	181	–	–	–	–	–

CS; crystal structure; OC; oxygen content.

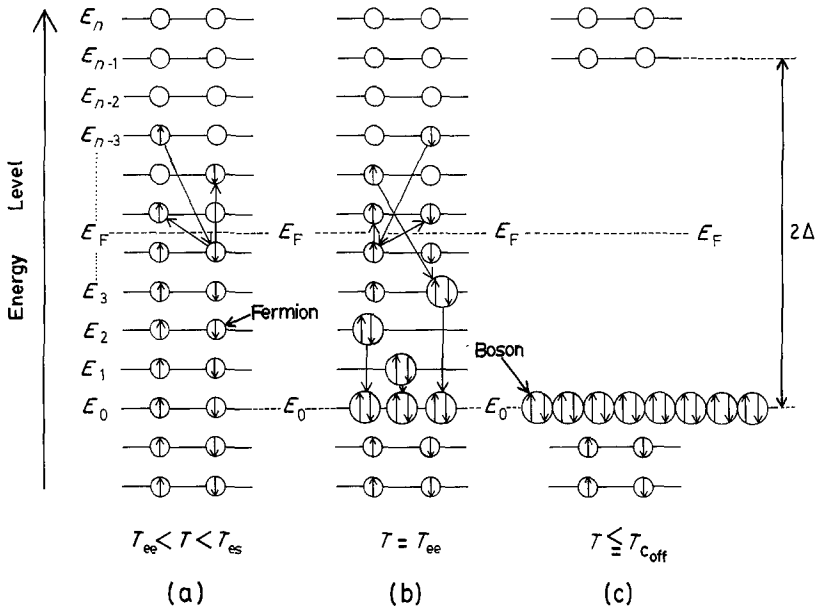

Figure 5 Schematic model of fermion and boson. (a) Electron–electron scattering between T_{es} and T_{ee} in Fig. 3, (b) model at lower critical temperature (T_{ee}; formation temperature of boson) of T^2 law, (c) model below $T_{c_{off}}$.

following equation:

$$T_{c_{off}} = 0.113T_{ee} + 69.9 \quad (5)$$

The slope and constant of Equation 5 are similar to those of Equation 4.

We have studied $T_{c_{off}}$ change with stress [18]. The stress increases $T_{c_{off}}$. Thus, we show the relationship between $T_{c_{off}}$ and T_{ee}, too, see Figure 11. The higher the T_{ee}, the higher the $T_{c_{off}}$ becomes, too. $T_{c_{off}}$ is expressed by the following equation:

$$T_{c_{off}} = 0.276T_{ee} + 43.9 \quad (6)$$

The slope of Equation 6 is about 2.7 ± 0.4 times larger than that of Equations 4 and 5. This shows that the effects of both the stress and solutes is not completely same, although the T_{ee}–$T_{c_{off}}$ law is applied as a general principle for the high T_c $YBa_2Cu_3O_{7-y}$ system. The results are consistent with the assumption that T_{ee} is the formation temperature of a boson.

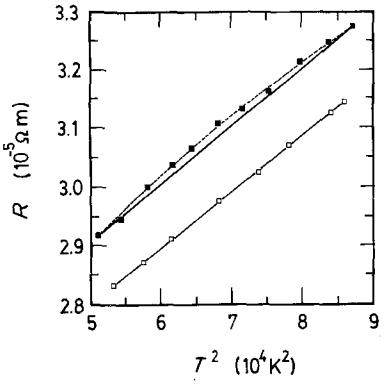

Figure 6 Change in electrical resistivity (R) with T^2 of $YBa_2Cu_3O_{7-y}$ system. (□) is for the measurement at equilibrium temperature: (■) is for the measurement under continous cooling conditions (scanning rate is 0.12 K sec^{-1}).

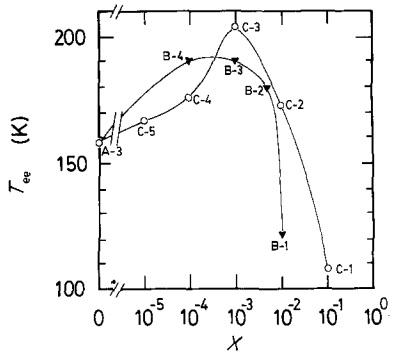

Figure 8 Change in lower critical temperature (T_{ee}; formation temperature of boson) of T^2 law with (○) Ti and (▼) Pd volume fraction (x) of $YBa_2(Cu_{1-x}Pd_x$ or $Ti_x)_3O_{7-y}$ system.

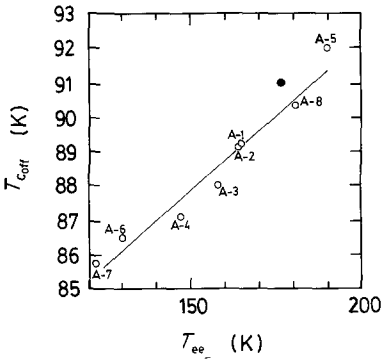

Figure 7 Relationship between offset temperature (T_{ee}) of T^2 law of $YBa_2Cu_3O_{7-y}$ system. (●) is for an oxygen processed sample. $T_{c_{off}} = 0.087$, $T_{ee} = 7.49$ K. 86 K < $T_{c_{off}}$ < 92 K, 122 K < T_{ee} < 190 K.

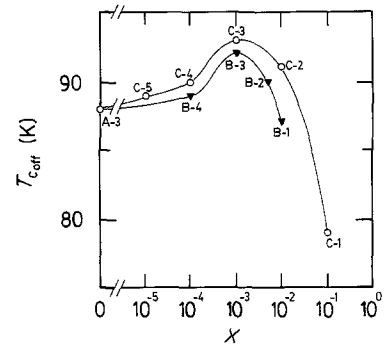

Figure 9 Change in offset temperature ($T_{c_{off}}$) of superconducting transition with (○) Ti and (▼) Pd volume fraction (x) of YBa_2-$(Cu_{1-x}Pd_x$ or $Ti_x)_3O_{7-y}$ system.

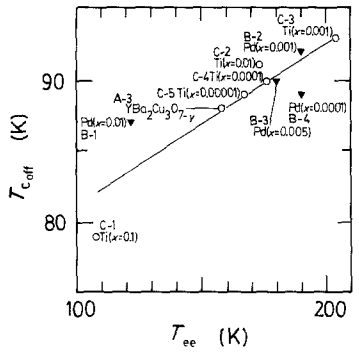

Figure 10 Relationship between offset temperature ($T_{c_{off}}$) of T^2 law of $YBa_2(Cu_{1-x}Pd_x$ or $Ti_x)_3O_{7-y}$ system. $T_{c_{off}} = 0.113\ T_{ee} + 69.9\,\mathrm{K}$. $79\,\mathrm{K} < T_{c_{off}} < 93\,\mathrm{K}$. $108\,\mathrm{K} < T_{ee} < 204\,\mathrm{K}$.

6. Conclusion

We investigated a lower critical temperature of T^2 law as the formation temperature of a boson for the high T_c $YBa_2Cu_3O_{7-y}$ system, where the electrical resistivity is measured at different equilibrium temperatures. The higher the T_{ee}, the higher the $T_{c_{off}}$ becomes. Therefore, we suggest that the $T_{ee}-T_{c_{off}}$ law is applied as a general principle for the high T_c $YBa_2Cu_3O_{7-y}$ system.

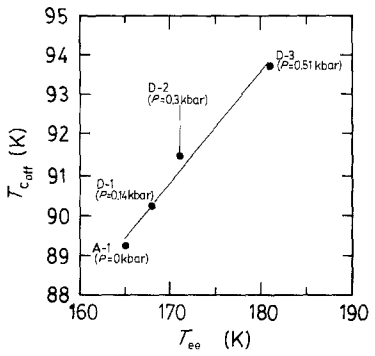

Figure 11 Relationship between offset temperature ($T_{c_{off}}$) and lower critical temperature (T_{ee}) of T^2 law of compressed $YBa_2Cu_3O_{7-y}$ system. $T_{c_{off}} = 0.276\ T_{ee} + 43.9\,\mathrm{K}$. $89\,\mathrm{K} < T_{c_{off}} < 94\,\mathrm{K}$. $165\,\mathrm{K} < T_{ee} < 181\,\mathrm{K}$.

References

1. M. K. WU, J. R. ASHBURN, C. J. TORNG, P. H. HOR, R. L. MERG, L. GAO, Z. J. HAUNG, Y. Q. WANG and C. W. CHU, *Phys. Rev. Lett.* **58** (1987) 908.
2. J. Z. SUN, D. J. WEBB, M. NAITO, K. CHAR, M. R. HAHN, J. W. P. HSU, A. D. KENT, D. B. MITZI, B. OH, M. R. BEASLEY, T. H. GEBALLE, R. H. HAMMOND and A. KAPITULNIK, *ibid.* **58** (1987) 1574.
3. Y. ZHONGJIN, Z. NAIPING, J. XIAOPING, P. DEXING, Q. HONGBO, S. GUOYUE, Z. ZE and Y. HUAFENG, *J. Phys. C.* **20** (1987) L351.
4. S. B. QADRI, L. E. TOTH, M. OSOFSKY, S. LAWRENCE, D. U. GUBSER and S. A. WOLF, *Phys. Rev. B.* **35** (1987) 7235.
5. J. M. TARASCON, W. R. McKINON, L. H. GREENE, G. W. HULL and E. M. VOGEL, *ibid.* **36** (1987) 226.
6. J. BARDEEN, L. N. COOPER and J. R. SCHRIEFFER, *Phys. Rev.* **108** (1957) 1175.
7. C. M. VARMA, S. SCHMITT-RINK and E. ABRAHAMS, *Solid State Commun.* **62** (1987) 681.
8. W. Y. CHING, Y. XU, G. L. ZHAO, K. W. WONG and F. ZANDIEHNADEM, *Phys. Rev. Lett.* **59** (1987) 1333.
9. P. W. ANDERSON, *Science* **235** (1987) 1196.
10. G. KRILL, *Solid State Commun.* **9** (1971) 1065.
11. B. LEVY, M. SINVANI and A. J. GREENFIELD, *Phys. Rev. Lett.* **43** (1979) 1822.
12. M. KHOSHNEISAN, W. P. PRATT Jr, P. A. SCHROEDER, S. STEENWYK and C. UHER, *J. Phys. F.* **9** (1979) L1.
13. L. LANDAU and I. POMERANCHUK, *Phys. Z. Sowjet.* **10** (1936) 649.
14. Y. NISHI, A. IGARASHI, S. TOKUNAGA and S. MORIYA, *J. Mater. Sci. Lett.* **7** (1988) 649.
15. Y. NISHI, unpublished data.
16. Y. NISHI, S. MORIYA and S. TOKUNAGA, *J. Mater. Sci. Lett.* **7** (1988) 359.
17. *Idem, Phys. Lett. A* **126** (1987) 55.
18. Y. NISHI, N. NINOMIYA and S. TOKUNAGA, *J. Mater. Sci. Lett.* **7** (1988) 361.

Received 3 October 1988
and accepted 13 April 1989